Biochemical and Biophysical Research Communications 407 (2011) 575–580

Contents lists available at ScienceDirect

Biochemical and Biophysical Research Communications

journal homepage: www.elsevier.com/locate/ybbrc

Cytokeratin 18-mediated disorganization of intermediate filaments is induced by degradation of plectin in human liver cells

Yi-Hsiang Liu [a,b], Chin-Chin Ho [c], Chiung-Chi Cheng [d], Wei-Ting Chao [e], Ren-Jeng Pei [f], Yung-Hsiang Hsu [b], Yih-Shyong Lai [a,*]

[a] Department of Pathology, Chang Bing Show Chwan Memorial Hospital, Changhua, Taiwan
[b] Department of Pathology, Tzu Chi University, Hualien, Taiwan
[c] Department of Nursing, Central Taiwan University of Science and Technology, Taichung, Taiwan
[d] Department of Medical Research, Chang Bing Show Chwan Memorial Hospital, Changhua, Taiwan
[e] Department of Molecular Physiology and Biophysics, Baylor College of Medicine, Houston, TX, USA
[f] Yongsin Pathological Center, Taichung, Taiwan

ARTICLE INFO

Article history:
Received 10 March 2011
Available online 21 March 2011

Keywords:
Cytokeratin
Cytoskeleton
Hepatocellular carcinoma
Plectin
Staurosporine
Transformation

ABSTRACT

Plectin is a cross-linking protein that organizes the cytoskeleton into a stable meshwork that helps maintain the uniform size and shape of cells. As cells of hepatocellular carcinoma are morphologically different from healthy human hepatocytes, we hypothesized that plectin deficiency and cytoskeletal disorganization underlies this pleomorphic transformation. To test this hypothesis we induced apoptosis as the most accessible pathway for creating plectin deficiency status *in vivo*. We analyzed expression levels and organization of plectin and other cytoskeletal elements, including intermediate filaments, microfilaments, and microtubules, after staurosporine-induced apoptosis in human Chang liver cells. The results revealed the expression of plectin and cytokeratin 18 were downregulated in hepatocellular carcinoma tissues *in vivo*. The expression of actin and tubulin, however, were not altered. *In vitro* analysis indicated that plectin and cytokeratin 18 were cleaved following staurosporine-treatment of human Chang liver cells. Time course experiments revealed that plectin was cleaved 2 h earlier than cytokeratin 18. The organization of plectin and cytokeratin 18 networks collapsed after staurosporine-treatment. Conclusively, degradation of plectin induced by staurosporine-treatment in liver cells resulted in cytoskeleton disruption and induced morphological changes in these cells by affecting the expression and organization of cytokeratin 18.

1. Introduction

The shape and structural integrity of human hepatocytes, like other animal cells, are maintained by the cytoskeleton. The cytoskeleton is composed of three organelles: intermediate filaments (IFs), microfilaments (MFs), and microtubules (MTs) [1]. IFs, with a diameter of 10 nm, are ropelike fibers consisting of members of a large heterogeneous family of proteins that includes cytokeratins (CKs) [2]. In human hepatocytes, the IF polymers are formed by a specific CK pair: CK8 (type II, molecular weight 52 kDa) and CK18 (type I, molecular weight 45 kDa) [3]. MFs are two-stranded helical polymers composed of actin with a diameter of 5–9 nm [4]. MTs are long, hollow cylinders composed of multiple isotypes of α- and β-tubulin with an outside diameter of 25 nm [5].

Proper cross-linking organization among cytoskeleton structures is critical for establishing the internal architecture and overall morphology of cells. Several cross-linking proteins that mediate the interaction between IFs and other cytoskeletal networks have been identified [2]. Among these, plectin is the most versatile. Plectin has binding sites for IF proteins, tubulin, and actin [6], and it is expressed in a variety of tissues and mammalian cell types [7,8]. At least one human disease has been attributed to altered plectin function; mutations in the plectin gene are the molecular basis of epidermolysis bullosa with muscular dystrophy [9]. The role of plectin deficiency in human cancer development, however, is largely unknown.

Abbreviations: MT, microtubule; MF, microfilament; IF, intermediate filament; CK, cytokeratin; IFAP, intermediate filament associated protein; HCC, hepatocellular carcinoma; HRP, horseradish peroxidase; DMEM, Dulbecco's minimum essential medium; FBS, fetal bovine serum; siRNA, small interfering RNA; PBS, phosphate-buffered saline; FITC, fluorescein-conjugated isothiocyanate; SDS, sodium dodecyl sulfate; PVDF, polyvinylidene fluoride; STS, staurosporine; DMSO, dimethyl sulfoxide; BSA, bovine serum albumin; SDS–PAGE, sodium dodecyl sulfate–polyacrylamide gel electrophoresis.

* Corresponding author. Address: Department of Pathology, Chang Bing Show Chwan Memorial Hospital, No. 6, Lugong Rd., Lugang Town, Changhua County 505, Taiwan. Fax: +886 4 7073235.
E-mail address: yslaick18@yahoo.com.tw (Y.-S. Lai).

0006-291X/$ - see front matter © 2011 Elsevier Inc. All rights reserved.
doi:10.1016/j.bbrc.2011.03.066

Hepatoma cells are morphologically distinctive from healthy liver cells. Therefore, we speculated that plectin deficiency might affect critical cytoskeletal elements, resulting in cytoskeletal disorganization and transformation of human liver cells. In our previous *in vivo* study, modulation of CK18 in human hepatocellular carcinoma (HCC) was established [10], and recently we found that plectin protein levels were reduced in human HCC tissues [11]. Based on RNA interference (RNAi), plectin knockdown in Chang liver cells decreases CK18 expression and results in the CK18 shrinkage phenotype; furthermore, actin-rich stress fibers are increased but the organization of microtubule networks is unaltered [12]. Based on these data, we confirmed that plectin regulates cytoskeletal organization and the overall architecture of human liver cells.

In considering the causes of plectin deficiency, apoptosis might be the most accessible pathway for creating plectin deficiency in cells. Several studies have demonstrated the degradation of plectin during apoptosis. For example, plectin can be a major early substrate for caspase 8 during CD95- and tumor necrosis factor receptor-mediated apoptosis [13]. In staurosporine (STS)-treated apoptotic HaCaT keratinocytes, plectin, desmoplakin, and periplakin are cleaved [14]. Another study has shown that during apoptosis, CK8/18 is reorganized into granular structures that facilitate the rapid collapse of the cytoskeletal architecture [15], and it has been recently demonstrated that colchicine-induced apoptosis results in cytoskeleton alterations [16]. These studies have indicated that plectin and the cytoskeleton are involved in apoptosis.

We previously found that STS-induced apoptosis in human Chang liver cells results in plectin cleavage and CK18 modulation as well as an unstable IF organization [17]. In that study, however, it was not apparent whether STS-treatment resulted in cleavage of plectin and CK18 or if CK18 cleavage occurred downstream of plectin degradation following STS-induced apoptosis. To clarify, in this study we observed the time course of plectin and CK18 cleavage during STS-induced apoptosis from 30 min to 7 h. In addition, we aimed to identify the influence of plectin degradation by STS-treatment on the expression and organization of the primary cytoskeletal elements (IFs, MFs, and MTs) and the overall morphology of liver cells. Human Chang liver cells were used as the experimental *in vitro* model. We also determined the *in vivo* expression of plectin, CK18, actin, and tubulin in human HCC and liver tissues. We also evaluated the *in vitro* and *in vivo* data to determine whether the effects of STS-induced plectin degradation were comparable to the *in vivo* status of plectin downregulation in human HCC.

2. Materials and methods

2.1. Tissue samples and antibodies

Fresh surgically resected HCC tissues from four patients with liver cancer and one patient with liver trauma were studied. All HCC cases were histopathologically diagnosed as grade II. These samples were stored at −80 °C before protein extraction and Western blot analysis. In addition, paraffin blocks from 10 cases of human grade II HCC were also obtained. The following commercial primary and secondary antibodies were used for immunohistochemistry, immunoblotting, and immunofluorescent assays: anti-CK18, anti-actin, and anti-tubulin monoclonal antibodies were purchased from Zymed Laboratories (South San Francisco, CA, USA); anti-plectin monoclonal antibody was purchased from Santa Cruz Biotechnology (Santa Cruz, CA, USA); anti-mouse and anti-goat IgG were purchased from Jackson ImmunoResearch Laboratories (West Grove, PA, USA). Anti-mouse and anti-goat IgG was conjugated to biotin for immunohistochemistry, to horseradish peroxidase (HRP) for Western blot analysis, and to rhodamine or fluorescein isothiocyanate (FITC) for immunofluorescent staining.

2.2. Immunohistochemistry

The deparaffinized and rehydrated sections were treated with 3% H_2O_2 for 10 min to eliminate endogenous peroxidase activity. Nonspecific binding sites were blocked with bovine serum albumin for 10 min. The sections were incubated with monoclonal antibodies against plectin (1:50 dilution), CK18 (1:100 dilution), actin (1:200 dilution), and tubulin (1:100 dilution) for 1 h at room temperature. The biotinylated anti-mouse and anti-goat IgG were added (1:400 dilution, for 1 h at room temperature), and the final signal was expressed using the avidin–biotin peroxidase technique in the presence of hydrogen peroxide [18]. These sections were evaluated under a light microscope (BX51; Olympus, Tokyo, Japan).

2.3. Cell culture and apoptosis induction

Chang human non-tumor liver cells were obtained from The American Type Culture Collection (ATCC; Rockville, MD, USA) number CCL-13. The cells were cultured in Dulbecco's minimum essential medium (DMEM; Invitrogen, Carlsbad, CA, USA) supplemented with 10% fetal bovine serum (FBS), 50 U/ml penicillin and streptomycin, and 200 mM L-glutamine. The medium was replaced every 2 days. The cells were subcultured as follows: for the immunoblotting analysis, 3×10^5 cells were seeded into 6-well tissue plates and for the immunofluorescence assay, 3×10^4 cells were grown on coverslips in 24-well tissue plates. At approximately 80% confluence, the medium was exchanged with new test medium containing 1 μM STS in dimethyl sulfoxide (DMSO), and the cells were incubated for 0.5, 1, 2, 3, 4, 5, 6, and 7 h for induction of apoptosis. Medium without STS was used as the negative control.

2.4. Quantification of apoptotic cells

The STS-treated cells on coverslips were washed with ice-cold phosphate-buffered saline (PBS; 137 mM NaCl, 2.7 mM KCl, 8 mM Na_2HPO_4, and 1.5 mM KH_2PO_4, pH 7.4) and fixed with 3% paraformaldehyde in PBS for 20 min at room temperature. After washing in PBS, the cells were permeabilized with 0.1% Triton X-100 in PBS for 2 min followed by three washes with cold PBS. The cells were then stained with 1 μg/ml 4,6-diamidino-2-phenylindole (DAPI) in PBS containing 1% bovine serum albumin (BSA) for 30 min at room temperature. After staining, the coverslips were washed three times with cold PBS, mounted on slides, and observed under a fluorescence microscope (BX51; Olympus, Tokyo, Japan). The fragmental nuclei of apoptotic cells were calculated from a total of 200 cells. We repeated the same experiments at least three times for quantitative analysis.

2.5. Immunofluorescence

Prior to staining, cells were washed with ice-cold PBS and fixed for 20 min with 3.7% paraformaldehyde/PBS at room temperature. After fixation, cells were washed three times with PBS and permeabilized with 0.1% Triton X-100/PBS for 2 min at room temperature. Cells were washed three times in PBS and double-stained for 60 min with primary antibodies at room temperature and then washed with PBS again. Cells were then incubated with rhodamine-conjugated anti-mouse IgG and FITC-conjugated anti-goat IgG secondary bodies for 30 min at room temperature. Finally, the unbound antibodies were removed by washing twice for

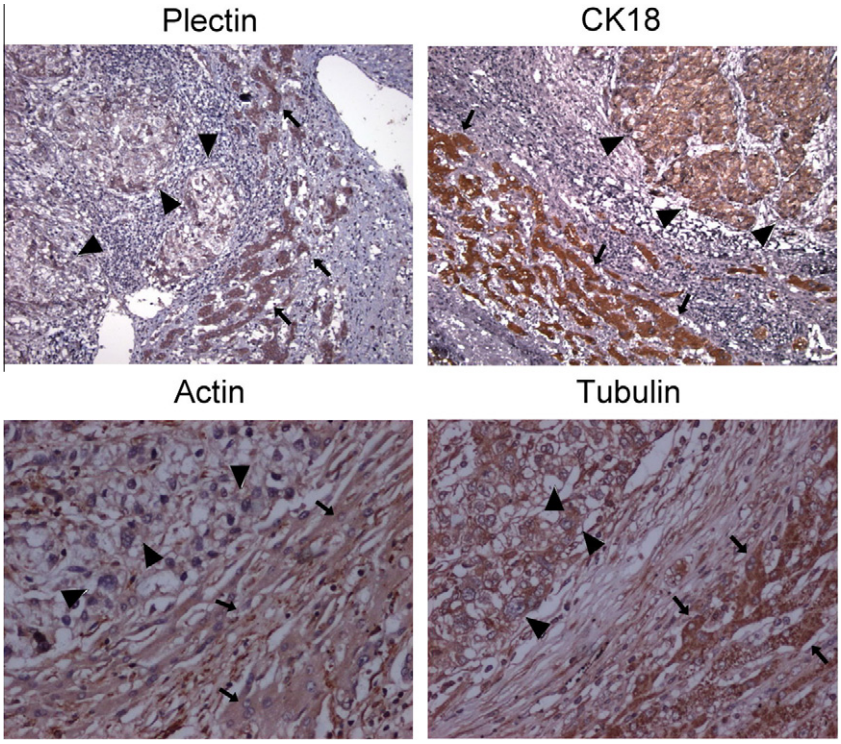

Fig. 1. The expression of plectin and cytoskeleton components in human non-tumor liver and HCC tissues by immunohistochemical staining. Plectin staining was strongly positive in the non-tumor regions of the HCC samples (arrow), while plectin staining was weak in the tumor regions (arrowhead). CK18 also revealed strong positive staining in the non-tumor regions (arrow), but the HCC tissues showed weak CK18 staining (arrowhead). The staining pattern of actin and tubulin was similar in HCC and non-tumor tissues. Arrowheads indicate HCC tissue, arrows indicate non-tumor tissue.

10 min in PBS [19]. The images were evaluated under a fluorescence microscope (BX51; Olympus, Tokyo, Japan).

2.6. Cytoskeleton extraction

In general, extractions were performed according to French's method [20]. Unless otherwise indicated, the preparation was conducted at 4 °C. Briefly, the minced specimen was first incubated with CSK buffer (300 mM sucrose, 3 mM $MgCl_2$, 0.5% Triton X-100, 10 mM piperazin-1,4-bis[2-ethanesulphonic acid], 1.2 mM phenylmethylsulfonyl fluoride, and 0.1 mM iodoacetamide) containing 100 mM NaCl for 5 min. After three washes, pellets were treated with CSK buffer containing 250 mM $(NH_4)_2SO_4$ for 10 min and then with the same buffer containing bovine pancreatic DNase I (100 μg/ml) and RNase A (100 μg/ml) for 10 min. Pellets were rinsed with the buffer containing DNase I, RNase A, and $(NH_4)_2SO_4$ for 10 min at room temperature. Finally, the preparation was resuspended in CSK buffer, and the concentration was adjusted to 1 mg/ml.

2.7. Western blot analysis

Protein extracts were prepared in sample buffer containing 0.5 M Tris–HCl (pH 6.8), 10% sodium dodecyl sulfate (SDS), 5% 2-mercaptoethanol, and 30% glycerol. Equal amounts of the extracted lysate (10 μg for CK18, actin, and tubulin electrophoresis; 40 μg for plectin electrophoresis) were separated by sodium dodecyl sulfate–polyacrylamide gel electrophoresis (SDS–PAGE; 6% for plectin, 10% for CK18, actin, and tubulin) [21]. After electrophoresis, proteins were transferred to polyvinylidene fluoride (PVDF) membranes using the semi-dry transfer method (Bio-Rad Laboratories, Hercules, CA, USA). Membranes were blocked for 1 h at room temperature (or 4 °C overnight) with a blocking buffer containing 5% (w/v) nonfat milk. Membranes were then incubated with monoclonal antibodies overnight at 4 °C (1:100 dilution for plectin, 1:200 dilution for CK18, 1:400 dilution for actin, 1:200 dilution for tubulin). Membranes were incubated with secondary antibodies (1:800 dilution) for 60 min at room temperature and visualized using enhanced chemiluminescence reagent (NEN Life Science Products, Boston, MA, USA).

3. Results

Ten human HCC tissue sections were processed for immunohistochemistry. The expression of plectin and CK18 in the HCC sections was clearly different when compared with the non-tumor tissues. As shown in Fig. 1, the tumor cells (arrowhead) were observed to be pleomorphic and arranged in irregular nests, and staining for plectin was weak. In the non-tumor tissues (arrow), the hepatocytes appeared as uniform cuboidal cells arranged in sheets or a plate pattern, and staining for plectin was strong. Also shown in Fig. 1, the expression of CK18 was observed to be dramatically different between HCC and non-tumor liver tissues. The staining for CK18 was strong in the non-tumor tissues (arrow). In contrast, the tumor tissues showed masses of pleomorphic and hyperchromatic tumor cells, and the staining for CK18 was weak (arrowhead). However, there was no difference between actin and tubulin expression in the HCC and non-tumor tissues (Fig. 1).

In order to confirm the above findings, Western blot analysis was performed on total protein extracts. After electrophoresis, differential expression of plectin was observed when comparing HCC and normal liver tissues. The zymogenic plectin migrated as a single band at approximately 300 kDa in the non-tumor liver tissue. In contrast, degraded plectin migrating at approximately 200 kDa was clearly present in the HCC tissues, and the levels of zymogenic plectin were markedly decreased (Fig. 2). Similarly, the expression

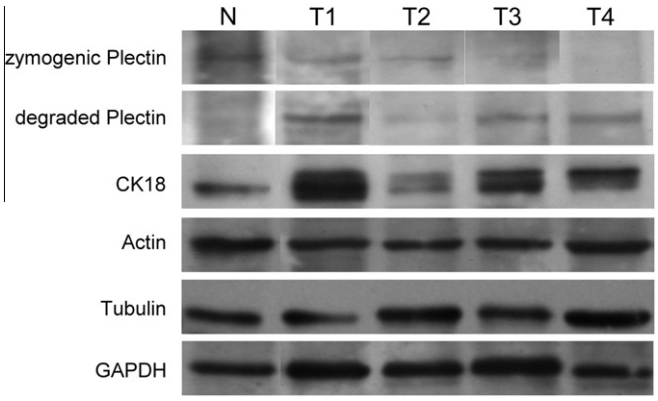

Fig. 2. The expression of plectin and cytoskeleton components in human non-tumor liver and HCC tissues by Western blot analysis. The expression of plectin was decreased in HCC tissues (T1–T4) compared with non-tumor liver tissues (N). CK18 migrated as two close bands in HCC tissues (T1–T4) compared to a single band in the non-tumor liver tissue (N). The expression of actin and tubulin revealed no difference between HCC and non-tumor liver tissues.

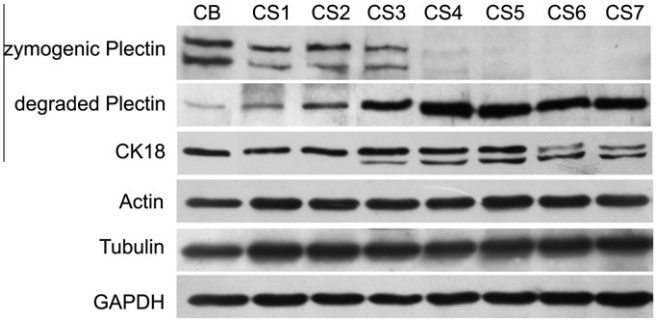

Fig. 3. Western blots analysis of plectin, CK18, actin, and tubulin with and without STS-treatment. Plectin and CK18 were cleaved following STS-treatment, but actin and tubulin were unchanged. GAPDH was used as an internal control.

of CK18 in the HCC tissue samples differed from that of the non-tumor liver tissues. Notably, CK18 in the non-tumor tissues migrated as one band, while CK18 in the tumor tissues ran as two bands with a higher molecular weight (Fig. 2). Meanwhile, the expression of actin and tubulin did not demonstrate any difference between HCC and non-tumor tissues in this analysis (Fig. 2). These results were consistent with the finding of the above immunohistochemistry investigation.

Based on Western blot analysis, zymogenic plectin from untreated liver cells (Fig. 3, CB) migrated at approximately 300–400 kDa, while degraded plectin (200 kDa) was present in the STS-treated cells (Fig. 3, CS1–CS7). These plectin cleavage products were observed at the 1-h time point (Fig. 3, CS1). The plectin was almost quantitatively cleaved between the 1- and 3-h time points and was almost completely cleaved after 4 h of STS-treatment (Fig. 3, CS4). Similarly, zymogenic CK18 migrated as a single band in the untreated cells (Fig. 3, CB), while two bands, including zymogenic CK18 and cleaved CK18, appeared after STS-treatment (Fig. 3, CS1–CS7). The cleaved CK18 was present at the 3-h time point (Fig. 3, CS3) and remained up to the 7-h time point (Fig. 3, CS7). In contrast, expression levels of actin and tubulin were unchanged, and no evidence of actin or tubulin cleavage was seen in the liver cells after STS-treatment. Comparison between the cleavage of plectin and CK18 revealed that initial cleavage of plectin occurred about 2 h earlier than that of CK18. Quantitative analysis revealed that the expression levels of plectin and CK18 were reduced by 95% and 60%, respectively, but that actin and tubulin levels were unaffected by STS-treatment (data not shown).

To investigate whether plectin was important for the organization of the cytoskeleton in liver cells, we compared cytoskeletal networks in control and plectin cleaved cells by immunofluorescence. As shown in Fig. 4, the plectin in the untreated cells was mainly distributed as a mesh structure in the perinuclear region and extended to the cell periphery in delicate filaments or in short, irregularly oriented fibers and dotted lines (control). CK18 was present in fine filament networks in the cytoplasm, with abundance in the perinuclear region, and mesh-like distributions extending toward the cell membrane (control). Plectin staining overlapped with CK18 staining in these cells, which indicated that plectin was colocalized with CK18 in human liver cells.

After STS-treatment, the characteristics of plectin and CK18 localization began to display a disrupted pattern and granular structure at 1 h after apoptosis induction (Fig. 4, 1H). The plectin mesh collapsed, concentrated in the perinuclear region, and showed a granular pattern. The CK18 networks redistributed as thick bundles of filaments and appeared to be retracted toward the nucleus. Collapse of the networks was evident, and disorganized thick filament bundles of tangled and clustered loop structures were observed. The networks seemed to be more densely compacted and had rearranged into rings and patches around the nucleus when compared with control cells. These phenomena were observed up to the 7-h time point (1H–7H). However, there were no obvious differences in the organization of MFs or MTs between the control and STS-treated cells (data not shown).

4. Discussion

The involvement of abnormal regulation of the cytoskeleton and associated proteins in human HCC was investigated in our laboratory. In this study, based on immunohistochemistry and

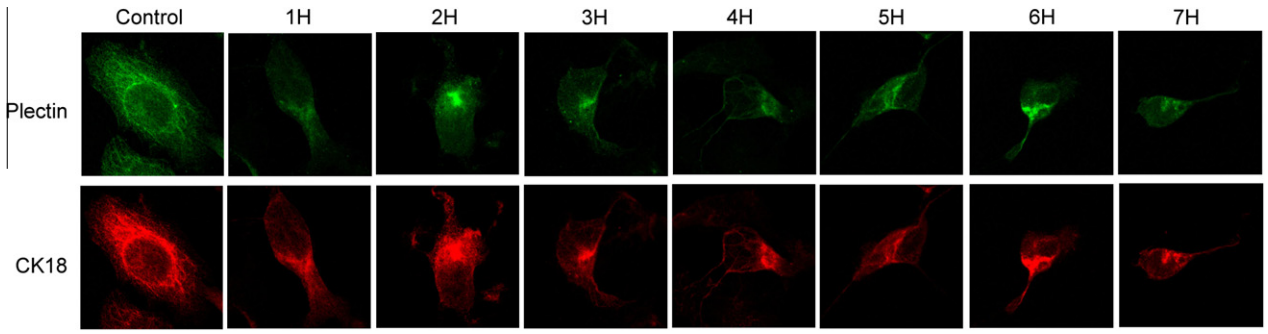

Fig. 4. Immunofluorescent assays for plectin and CK18 in Chang liver cells after STS-treatment. In untreated cells (control), plectin and CK18 were mainly distributed as mesh structures in the perinuclear region and extended to the membrane. In STS-treated cells (1H–7H), plectin and CK18 demonstrated dramatic morphological changes, with collapse of plectin and CK18 structures.

immunoblot analysis, we found that the *in vivo* expression of plectin was downregulated in HCC tissues compared with paired non-tumor liver tissues. The expression of CK18 was also modulated in HCC tissues. The expression of actin and tubulin, however, was not altered in HCC tissues. *In vitro* analysis indicated that plectin and CK18 were cleaved following STS-treatment of human Chang liver cells. Time course experiments revealed that plectin was cleaved 2 h earlier than CK18. In contrast, actin and tubulin were not affected by STS-treatment. Based on immunofluorescent observations, the morphology of human Chang liver cells changed following STS-induced apoptosis, and the organization of plectin and CK18 networks were also shown to have collapsed. These *in vitro* findings were compatible with our previous study indicating that the expression and organization of CK18, but not that of actin or tubulin, were altered following knockdown of plectin via RNAi in human Chang liver cells [12].

Abnormal regulation of the cytoskeleton as well as its associated proteins has been investigated in several neoplasms. For example, downregulation of CK19 in oral squamous cell carcinoma [22], downregulation of MFs and their binding protein gelsolin in breast cancer [23], and upregulation of tenascin-C and vimentin in breast cancer [24] have all been documented. In addition, the relationship between cytoskeletal structure and the pleomorphism of cancer cells was confirmed when alterations in cell shape of the human prostate cancer cell line DU145 were shown to be regulated by MFs based on electron microscopy [25]. The involvement of cytoskeleton regulation in the morphological change, invasion, and carcinogenesis of cancer cells was also raised in these previous studies. It is our view that pleomorphism of human HCC cells might be related to the downregulation of plectin and CK18, as we observed that these two proteins are both downregulated in human HCC tissue *in vivo*. In addition, we propose that actin and tubulin are not involved in the cellular pleomorphism of HCC cells, as we found the expression of actin and tubulin was unchanged in these cancer cells.

Degradation or downregulation of plectin in cells likely abolishes its ability to cross-link cytoskeletal elements, resulting in disorganization of the cytoskeleton and cellular pleomorphism. Previously we found STS-induced apoptosis in human Chang liver cells resulted in plectin and CK18 cleavage as well as morphological changes [17]. In this current study, we further confirmed that CK18 cleavage occurred downstream of plectin cleavage following STS-treatment. Thus, cleavage of plectin prior to degradation of CK18 might promote morphological changes in human liver cells. An analogous phenomenon was observed by other researchers who reported that plectin was cleaved by caspase 8 in the MCF7 human breast carcinoma cell line, which preceded cleavage of other caspase substrates including CK18 [13], and this is likely involved in the profound morphological alterations observed during apoptosis.

In this current study, plectin was found to be downregulated and cleaved in human HCC tissues *in vivo*. STS-induced apoptosis in healthy liver cells mimicked our *in vivo* observations indicating degradation of plectin, modulation of CK18, disrupted organization of CK18, and the presence of transformed cell morphology. Meanwhile, we observed that the expression of actin and tubulin was not altered after STS-treatment. These results were analogous to our *in vivo* data and supported our speculation that plectin deficiency affected the expression and organization of CK18, subsequently inducing morphological changes within human liver cells; actin and tubulin, however, were not involved in this process. A similar phenomenon was demonstrated by other investigators, as they showed that in STS-treated apoptotic HaCaT keratinocytes, plectin, desmoplakin, and periplakin are coordinately cleaved following the elimination of CK10 and 14, while actin and involucrin displayed considerable stability [14]. As such, we concluded that the effects of plectin degradation in human liver cells do not influence all three main cytoskeletal components, but rather that CK18 is a unique target of plectin degradation.

The *in vivo* mechanism underlying plectin deficiency in human HCC is unclear. We speculate that it might be associated with apoptosis-related plectin degradation, as plectin is a major early *in vivo* substrate for caspase 8 during CD95- and tumor necrosis factor receptor-mediated apoptosis [13]. Liver cell plectin in rats is also the substrate of μ-calpain, and the degradation of plectin could be an important event in the destabilization of hepatoma cells [26]. We demonstrated the degradation of plectin and modulated expression of CK18 in human liver cells during STS-induced apoptosis. Together, these data suggested that apoptosis-related protein degradation might be involved in plectin deficiency in human HCC. Exploring the exact mechanism of plectin deficiency in human HCC is the goal of future experiments.

In conclusion, we have confirmed that plectin regulates the cytoskeletal organization and the overall architecture of human liver cells. Degradation of plectin following STS-treatment in these cells affected the expression and organization of CK18, partially disrupted the architecture of the cytoskeleton, and induced pleomorphic changes that may be conserved in human HCC.

References

[1] G. Feldmann, The cytoskeleton of the hepatocyte. Structure and functions, J. Hepatol. 8 (1989) 380–386.

[2] E. Fuchs, D.W. Cleveland, A structural scaffolding of intermediate filaments in health and disease, Science (New York, NY) 279 (1998) 514–519.

[3] P. Van Eyken, V.J. Desmet, Cytokeratins and the liver, Liver 13 (1993) 113–122.

[4] N. Volkmann, D. DeRosier, P. Matsudaira, D. Hanein, An atomic model of actin filaments cross-linked by fimbrin and its implications for bundle assembly and function, J. Cell Biol. 153 (2001) 947–956.

[5] E. Nogales, Structural insights into microtubule function, Annu. Rev. Biochem. 69 (2000) 277–302.

[6] G.A. Rezniczek, L. Janda, G. Wiche, Plectin, Methods Cell Biol. 78 (2004) 721–755.

[7] S. Kazerounian, J. Uitto, S. Aho, Unique role for the periplakin tail in intermediate filament association: specific binding to keratin 8 and vimentin, Exp. Dermatol. 11 (2002) 428–438.

[8] G. Wiche, Role of plectin in cytoskeleton organization and dynamics, J. Cell Sci. 111 (Pt. 17) (1998) 2477–2486.

[9] R. Schröder, W.S. Kunz, F. Rouan, et al., Disorganization of the desmin cytoskeleton and mitochondrial dysfunction in plectin-related epidermolysis bullosa simplex with muscular dystrophy, J. Neuropathol. Exp. Neurol. 61 (2002) 520–530.

[10] B. Su, R.J. Pei, K.T. Yeh, et al., Could the cytokeratin molecule be modulated during tumor transformation in hepatocellular carcinoma?, Pathobiology 62 (1994) 155–159

[11] C.C. Cheng, Y.H. Liu, C.C. Ho, et al., The influence of plectin deficiency on stability of cytokeratin18 in hepatocellular carcinoma, J. Mol. Histol. 39 (2008) 209–216.

[12] Y.H. Liu, C.C. Cheng, C.C. Ho, et al., Plectin deficiency on cytoskeletal disorganization and transformation of human liver cells in vitro, Med. Mol. Morphol. 44 (2011) 21–26.

[13] A.H. Stegh, H. Herrmann, S. Lampel, et al., Identification of the cytolinker plectin as a major early in vivo substrate for caspase 8 during CD95- and tumor necrosis factor receptor-mediated apoptosis, Mol. Cell. Biol. 20 (2000) 5665–5679.

[14] S. Aho, Plakin proteins are coordinately cleaved during apoptosis but preferentially through the action of different caspases, Exp. Dermatol. 13 (2004) 700–707.

[15] B. Schutte, M. Henfling, W. Kolgen, et al., Keratin 8/18 breakdown and reorganization during apoptosis, Exp. Cell Res. 297 (2004) 11–26.

[16] E.G. Jordà, E. Verdaguer, A. Jimenez, et al., Evaluation of the neuronal apoptotic pathways involved in cytoskeletal disruption-induced apoptosis, Biochem. Pharmacol. 70 (2005) 470–480.

[17] Y.H. Liu, C.C. Cheng, C.C. Ho, et al., Degradation of plectin with modulation of cytokeratin 18 in human liver cells during staurosporine-induced apoptosis, In Vivo 22 (2008) 543–548.

[18] S.M. Hsu, L. Raine, H. Fanger, Use of avidin–biotin–peroxidase complex (ABC) in immunoperoxidase techniques: a comparison between ABC and unlabeled antibody (PAP) procedures, J. Histochem. Cytochem. 29 (1981) 577–580.

[19] K.H. Reuner, P. Dunker, A. van der Does, M. Wiederhold, I. Just, K. Aktories, N. Katz, Regulation of actin synthesis in rat hepatocytes by cytoskeletal rearrangements, Eur. J. Cell Biol. 69 (1996) 189–196.

[20] Y. Katsuma, N. Marceau, M. Ohta, S.W. French, Cytokeratin intermediate filaments of rat hepatocytes: different cytoskeletal domains and their three dimensional structure, Hepatology 8 (1988) 559–568.
[21] U.K. Laemmli, Cleavage of structural proteins during the assembly of the head of bacteriophage T4, Nature 227 (1970) 680–685.
[22] D.L. Crowe, G.E. Milo, C.F. Shuler, Keratin 19 downregulation by oral squamous cell carcinoma lines increases invasive potential, J. Dent. Res. 78 (1999) 1256–1263.
[23] H.L. Asch, K. Head, Y. Dong, et al., Widespread loss of gelsolin in breast cancers of humans, mice, and rats, Cancer Res. 56 (1996) 4841–4845.
[24] N. Dandachi, C. Hauser-Kronberger, E. More, et al., Co-expression of tenascin-C and vimentin in human breast cancer cells indicates phenotypic transdifferentiation during tumour progression: correlation with histopathological parameters, hormone receptors, and oncoproteins, J. Pathol. 193 (2001) 181–189.
[25] J. Chakraborty, G.A. Von Stein, Pleomorphism of human prostatic cancer cells (DU 145) in culture—the role of cytoskeleton, Exp. Mol. Pathol. 44 (1986) 235–245.
[26] M. Muenchbach, M. Dell'Ambrogio, P. Gazzotti, Proteolysis of liver plectin by mu-calpain, Biochem. Biophys. Res. Commun. 249 (1998) 304–306.